Application of the wavelet transform to analysis of the spatiotemporal structure of wind velocity fields

A.L. Afanasiev and V.A. Banakh

Institute of Atmospheric Optics,
Siberian Branch of the Russian Academy of Sciences, Tomsk

Received December 22, 2005

Time series of wind velocity measured with a Doppler lidar at different altitudes have been analyzed using the local coherence function of the wavelet transforms of signals (*Izvestiya RAN, Atmospheric and Oceanic Physics* **37**, No. 5, 584–591 (2001)). Feasibility of isolating groups of wind data with the coordinated behavior is demonstrated using a particular measurement session. It is shown that the coherence function allows one to isolate 2-D time–frequency domains with the high correlation of the wind velocity data upon the preliminary compensation for the local phase shifts of the same scale. The approach considered can be used for the detection and study of the dynamics of coherent formations in the atmosphere.

Introduction

The investigation into the spatiotemporal structure of the 3-D wind velocity fields in the atmosphere is mostly based on the statistical analysis of the series of measurement data compiled: calculations of the mutual correlation functions, mutual spectra, coherence and phase spectra, etc. The basic mathematical instrument used in the processing and study of the signal structure in this case is the Fourier transform. Due to the efficient computational algorithms of the Fast Fourier Transform,[1] the spectral approach finds a very wide application in the analysis of experimental data.

However, along with the obvious advantages, the Fourier-transform analysis has certain disadvantages if applied to treatment of the atmospheric processes. In particular, the assumption of steady-state processes is required. The problem of assessing the influence of the finiteness of the measured data series arises too. In this case, all possible trends are the interfering factors and usually these ought to be eliminated at the stage of preliminary processing of the measurement data. Therefore, all dynamic changes in the statistics of a process within a considered finite-length realization appear to be averaged. This, in turn, imposes increased demands on the selection of the length of realization and time of averaging in analyzing specific data.

The spatial inhomogeneity and unsteady character are most pronounced in the study of the structure of wind velocity fields in the region of scales, corresponding to the energy range of the turbulence spectrum. At the same time, numerous experimental data obtained in the past decades (including images taken from space) show that large-scale ordered eddies, referred to as coherent structures, play an important role in the natural and simulated turbulent flows. The examples of such eddies are, for instance, "cloud streets" in the atmosphere, "Langmuir circulations" in seas and lakes, periodic large eddies in jets of jet engines, etc.

It turned out that coherent structures are the main energy carriers in turbulent flows. They considerably affect the formation of all characteristics of a flow, in particular, the heat and mass exchange, transport of pollutants and momentum, sound excitation, etc. Coherent structures may be formed, under certain conditions, in turbulent flows at the expense of the flow energy (energy-carrying eddies), and then collapse, dissipating into chaotic motion. They also may, on the contrary, consume the energy of the turbulent motion in the flow for their existence (dissipative eddies).[2–6] These facts are beyond the common ideas about the absolute chaotic nature of turbulent motions and the cascade mechanism of the energy transfer from large scales to small scales. It becomes necessary to search for new approaches and methods for interpreting experimental results.

Recently, the method of wavelet transform has found wide application to analysis of experimental data on atmospheric processes.[7] This method allows random signals to be presented in the form of a function of two variables: time (shift) and time scale (period or frequency) that enables one to study then local properties of their frequency–time structure. The wavelet analysis is used in studying unsteady atmospheric processes[8] and allows one to identify and analyze coherent structures in the atmosphere,[9–11] as well as to reveal the periodicity in long-term series of observation data on atmospheric parameters.[12] Along with the traditional application of wavelet transforms, new methods of their application to analysis of geophysical data are now being developed.[11,12]

In this paper, we use the wavelet-based method of investigation of local characteristics of random

0235-6880/06/07 540-07 $02.00

processes proposed in Ref. 12 to analyze data on wind velocity in the atmosphere, obtained with the use of a coherent Doppler lidar.[13] This method permits the joint analysis of many-point observation series and separation of regular components with the time and scale localization.

1. Basic relationships

The wavelet transform of the function $f(t)$ is defined as its integral transformation with the kernel Φ

$$\Psi(s,\tau) = s^{-1/2}\int_{-\infty}^{\infty} f(t)\Phi\left(\frac{t-\tau}{s}\right)\mathrm{d}t, \qquad (1)$$

where $\Phi(\xi)$ is the wavelet function. In this paper, we used the wavelet of the "Mexican hat" type[7]:

$$\Phi(\xi) = (\xi^2 - 1)\exp(-\xi^2/2),$$

which allows maxima and minima in the signal to be isolated quite well.

We define some characteristics of the relation between two signals in terms of their wavelet transforms.[12] Let f_1 and f_2 be two signals, while Ψ_1 and Ψ_2 be their wavelet transforms on some scale s, and, correspondingly, τ'_i and τ''_j are points of local extremums of Ψ_1 and Ψ_2. The local phase shift of these signals on the scale s for the local extreme τ'_i, according to Ref. 12, is

$$l_{1,2}(\tau'_i, s) = \min_j(\tau'_i - \tau''_j), \qquad (2)$$

where $\tau''_j \in (\tau'_i - s/2,\ \tau'_i + s/2)$.

For each extremum τ'_i of the function Ψ_1, the closest extremum (maximum or minimum) point of the function Ψ_2 is sought within the s-wide vicinity near the point τ'_i. The local phase shift for zeros of the wavelet transform is determined in similarly. This definition allows the phases of oscillations of the scale s in the vicinity of maximum deviations to be compared and the phase changes at intermediate points to be ignored.

The local coherence function is determined as a correlation coefficient of the wavelet transforms of this couple of signals on the scale s for the points, at which the function $l_{1,2}(\tau, s)$ is defined, by the following equation[12]:

$$Coh_{1,2}(\tau, s; l_{1,2}) = \frac{\int_{\tau-s/2}^{\tau+s/2}\Psi_1(s,t)\Psi_2[s, t + l_{1,2}(\tau,s)]\mathrm{d}t}{\left\{\int_{\tau-s/2}^{\tau+s/2}\Psi^2{}_1(s,t)\mathrm{d}t\int_{\tau-s/2}^{\tau+s/2}\Psi^2{}_2[s,t+l_{1,2}(\tau,s)]\mathrm{d}t\right\}^{1/2}}. \qquad (3)$$

The definitions introduced give the possibility of estimating the phase characteristics and coherence of the signals studied not only for periodic components, but also for individual perturbations of the corresponding scale s.

2. Case study example

The main qualitative features of the analysis method used can be demonstrated with two test signals f_1 and f_2, taken as an example. Each of these signals consists of a sum of three frequency-separated sinusoidal signals of a unit amplitude. The initial phase for each component of the signals was specified in the interval from $-\pi$ to $+\pi$ with the aid of a random number generator. An example of realization of such signals is shown in Fig. 1.

Figure 2 depicts the wavelet transforms (1) of these signals. In the plot, the minimum values of the wavelet coefficients are shown by white color, the maximum ones are shown by black, and all the intermediate values are given in the gray scale.

In the frequency–time plane of the plots, one can see the positions of maxima and minima for each of the three components of the signals, corresponding to certain frequencies. The relative positions of the extremums of the functions f_1 and f_2 on the time axis correspond to the initial phase shifts of the signal components.

Figure 3 shows the local phase shifts, found according to Eq. (2) in the entire frequency–time plane for the given pair of wavelet transforms. On the scale (frequency) axis, the positions of the constant values of local shifts are concentrated around three frequencies, corresponding to the three components of the test signals f_1 and f_2. This is clearly seen in Fig. 3*b*, which shows only the shifts at these three scales. For each of the three frequency components, the local shift remains nearly constant all over the time axis.

Figure 4 depicts the local shifts of the wavelet coefficients, measured in units of the discretization step on the sales, corresponding to the frequencies of the components of the test signals. The time deviations occurring in the shift values can be attributed to the calculation errors, caused by the fact that the positions of local extremums (2) and points of intersecting zero are determined accurate to one step of the signal discretization. Therefore, in the central part of the time axis, these errors are larger for the high-frequency component than for the low-frequency one. At the origin and at the end of the time axis, the accuracy of calculations is also influenced by the edge effects, inherent in wavelet transforms at the realization domain boundaries. These distortions are more pronounced for the low-frequency component of the signal.

Figure 5*a* shows the values of the local coherence, calculated by Eq. (3) without the local adjustment of the phases of the signal components (shifts $l_{1,2}(\tau'_i, s) = 0$). It can be seen that the local coherence function of the two test signals in the time–scale plane has a periodic structure, characteristic of signals with the constant (in time) phase difference,

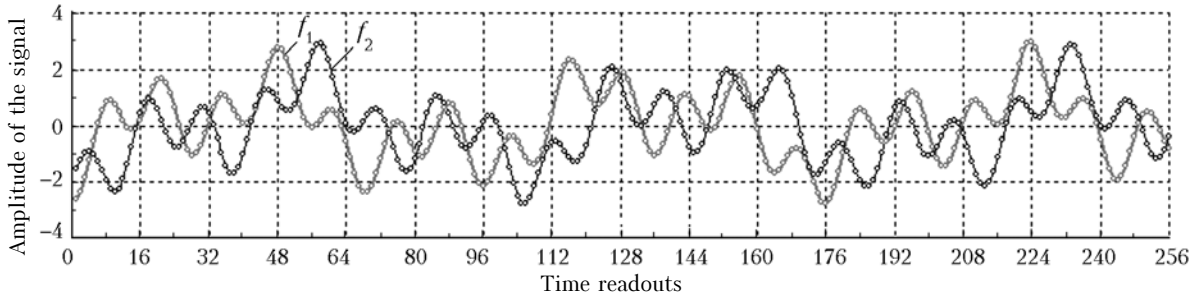

Fig. 1. Signals f_1 and f_2.

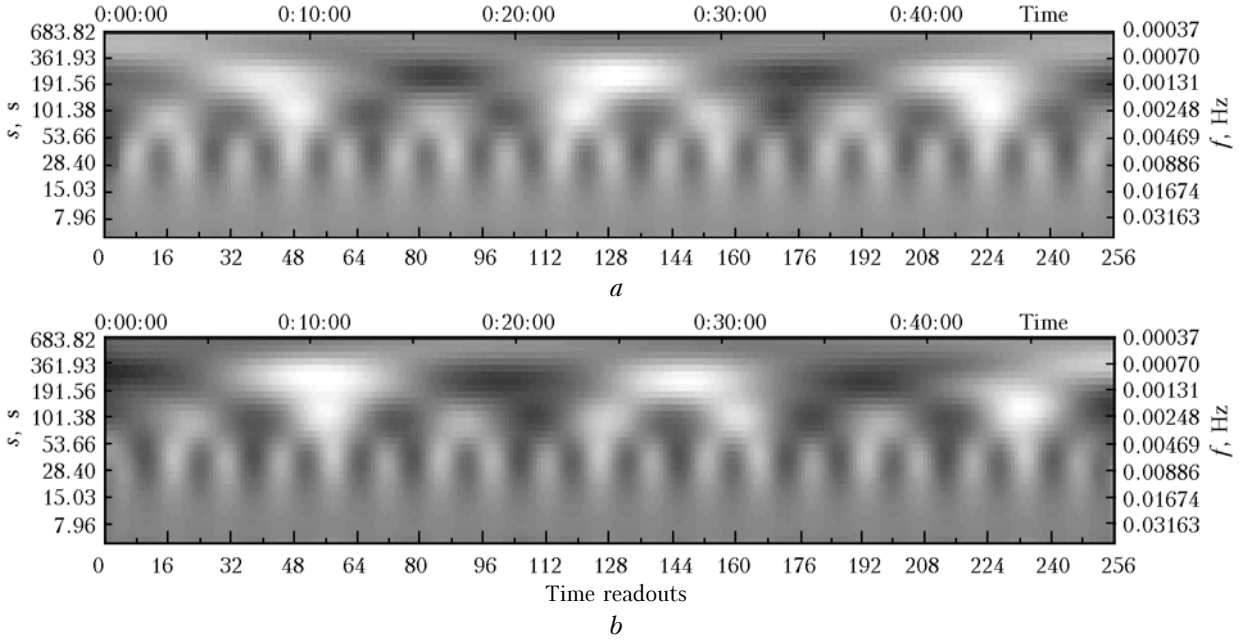

Fig. 2. Wavelet transforms of the signals f_1 (*a*) and f_2 (*b*).

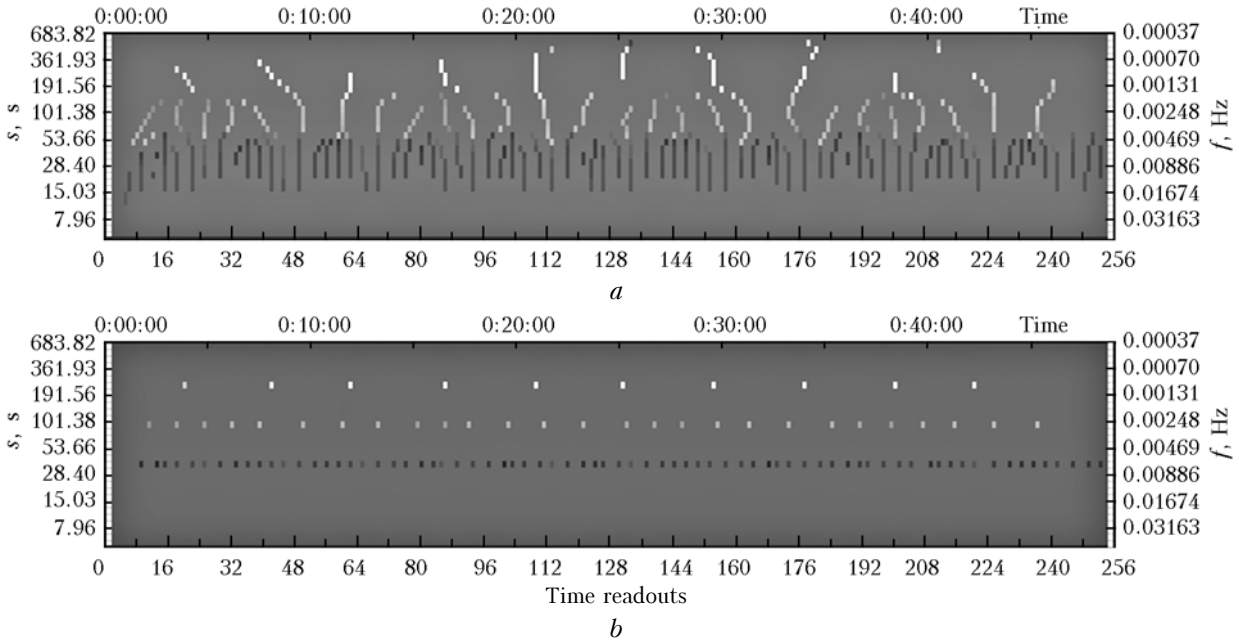

Fig. 3. Local phase shifts of the wavelet transforms of the signals f_1 and f_2: (*a*) for any scale; (*b*) for the scales, corresponding to the frequency components of the test signals.

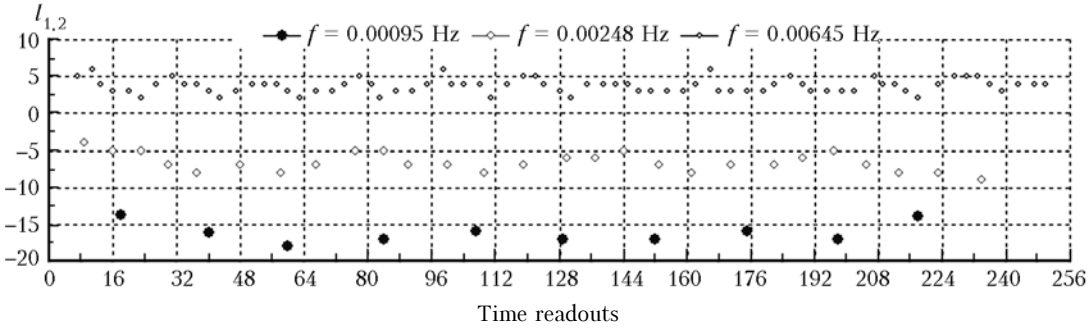

Fig. 4. Local shifts of the wavelet coefficients at the frequencies of the components of the test signals.

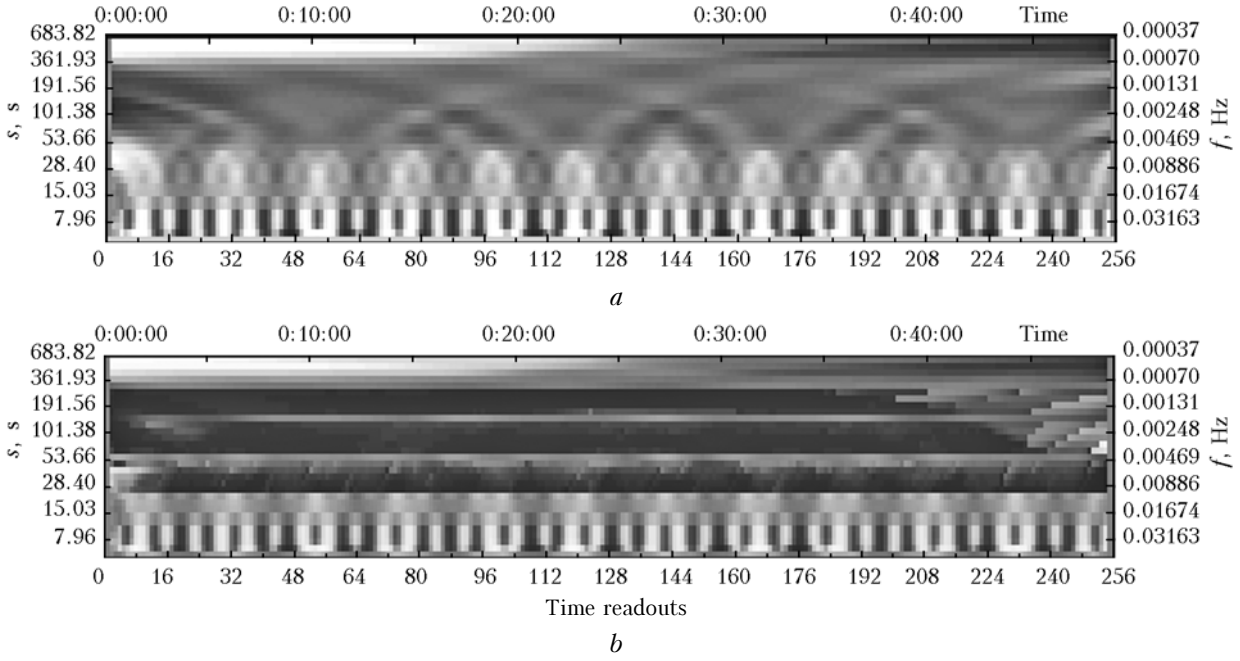

Fig. 5. Local coherence of the wavelet transforms of the test signals without (*a*) and with (*b*) adjustment of phases.

that is, for coherent signals. Unlike the Fourier transform, the wavelet transform of a harmonic signal is not a delta function, but occupies some band of the scales s, whose width is determined by the frequency resolution of the transform. In the wavelet plane, the bands, occupied by the frequency components of the signal, partly overlap. Because of the overlap, the local coherence calculated by Eq. (3) on a specific scale takes the periodically changing values depending on time. To find the ranges of the scales with high coherence, it is necessary to carry out local adjustment of the phases of oscillations on some scale or a range of scales.

Figure 5*b* shows the frequency–time structure of the local coherence, calculated with the local phase adjustment near the initial frequencies of the components of the test signals. For this purpose, the local shifts calculated previously (see Fig. 3*a*) were used in Eq. (3). In contrast to Fig. 5*a*, in Fig. 5*b* we can see three ranges of scales with the high coherence on the whole time axis, and just these ranges are the darkest ranges, in which the coherence values are close to unity.

Thus, from the local coherence function of the wavelet transforms of the signals with the compensation for their phase shifts, it is possible to reveal the regular components of these signals and to determine their location.

3. Application to processing experimental data

Consider the application of the method to processing atmospheric signals. Figure 6 shows the wind velocity V_1 and V_2 measured with a Doppler lidar at a distance of 650 and 1000 m from the lidar along the direction of propagation of the sounding beam.[13] Actually, we consider the realizations of the wind velocity measured at the points, separated by 350 m in the vertical plane along the direction at some scanning angle.[13] The realizations V_1 and V_2 consist of 256 points with the interval of 11.5 s between the readouts. That is, the signal discretization frequency is $f_d = 0.0869$ Hz, and the duration of the realization is 49 min. The wavelet transforms of the signals V_1 and V_2 are shown

in Fig. 7. The maximum frequency corresponds to $f_d/2$.

The local phase shift was calculated by Eq. (2) accurate to one signal discretization step. Since $f_d = 0.0869$ Hz, the relative time shift between the phases of the spectral components of the two signals is determined accurate to $\Delta_l = l/f_d = 11.5$ s. The error in determination of the phase shift with respect to the period of the spectral component for the high-frequency components of the signals, as was mentioned above, appears to be larger than for the low-frequency ones. In Fig. 8, for the component with the shortest period $T_{min} = 2/f_d$, the maximum value of the relative error of determination of the local phase shift is $\Delta_l/T_{min} = 50\%$. Correspondingly, for the component with the longest period, present in the range under consideration, the error is $\Delta_l/T_{min} = 0.5\%$. Figure 8 shows the distribution of the local phase shifts $l_{1,2}$. The white color corresponds to the maximum negative values of the local shifts, and the black color corresponds to the maximum positive shifts.

Figure 9*a* shows the local coherence function of the wavelet transforms of the signals V_1 and V_2 without phase adjustment (with zero shifts).

Except for the upper part of Fig. 9*a*, where the synchronism of the low-frequency trend in both of the signals manifests itself on the scales, comparable with the length of realization, the dark areas (with the high coherence) occupy only small parts in the scale–time coordinates and are separated by white (noncoherent) bars. In the central part of the considered range of scales, one fails to see extended (in time) areas with high coherence.

Figure 9*b* shows the coherence function calculated by Eq. (3) with the use of the local adjustment of the signal phases, that is, with the use of the shifts shown in Fig. 8. We can see that after the local adjustment of the phases the wavelet transforms in the scale range from 60 to 180 s in the vicinity of the corresponding points τ'_i and $\tau'_i \pm l_{1,2}(\tau'_i, s)$ appear to be coherent almost through the entire time period under consideration. That is, the local coherence function takes the limiting values of 1 and 0 at a rather large part of the frequency–time plane, colored in black for $Coh_{1,2}(\tau, s; l_{1,2}) = 1$ and white for $Coh_{1,2}(\tau, s; l_{1,2}) = 0$. The value of the local coherence as applied to the wind velocity can be treated as a measure of stability of the velocity eddy.[2]

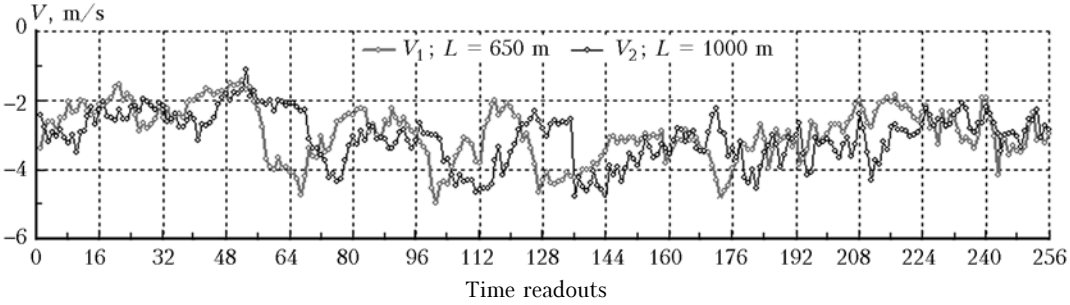

Fig. 6. Wind velocity realizations V_1 and V_2.

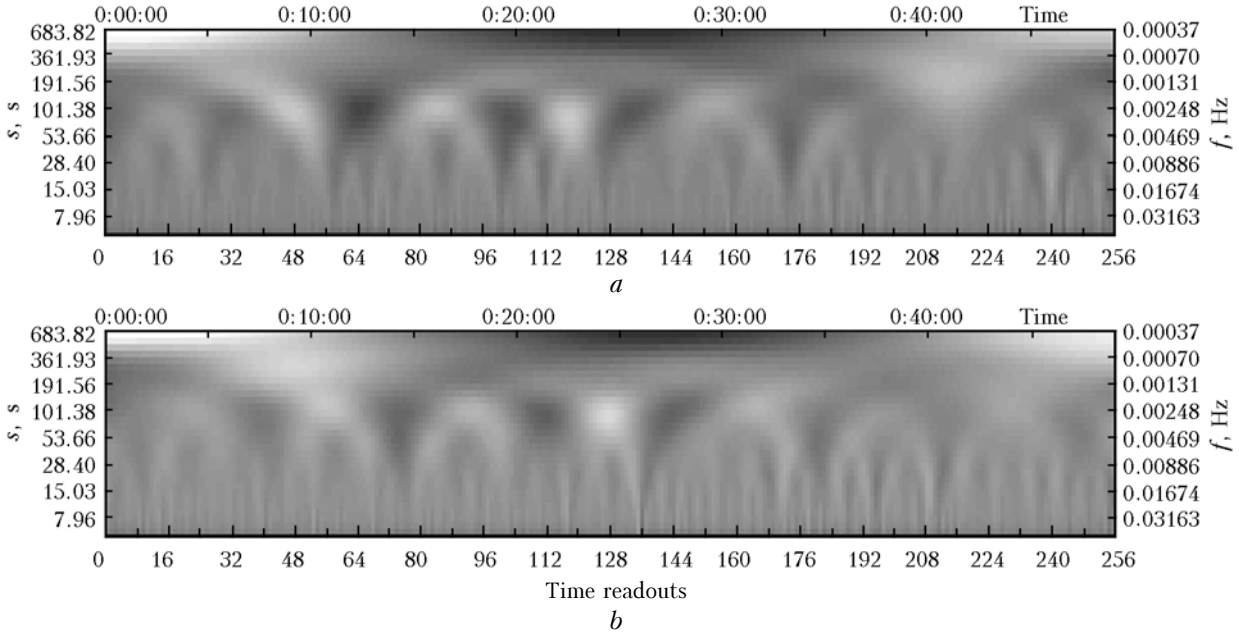

Fig. 7. Wavelet transforms of the signals V_1 (*a*) and V_2 (*b*).

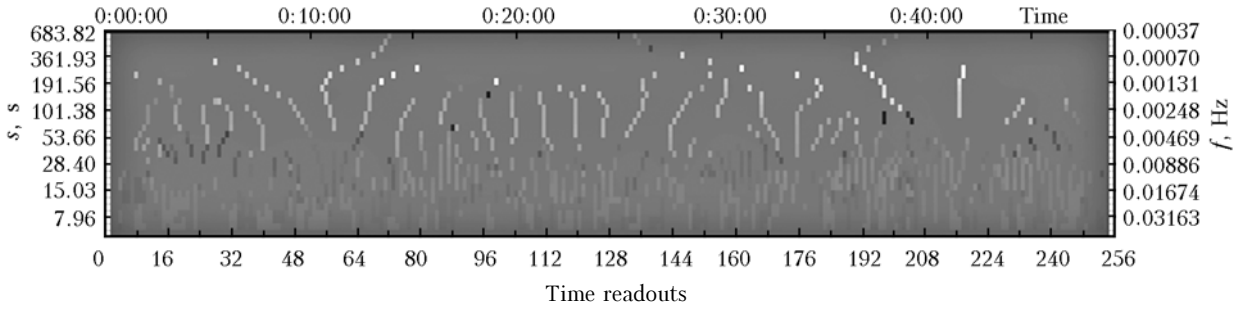

Fig. 8. Local phase shifts of the signals V_1 and V_2.

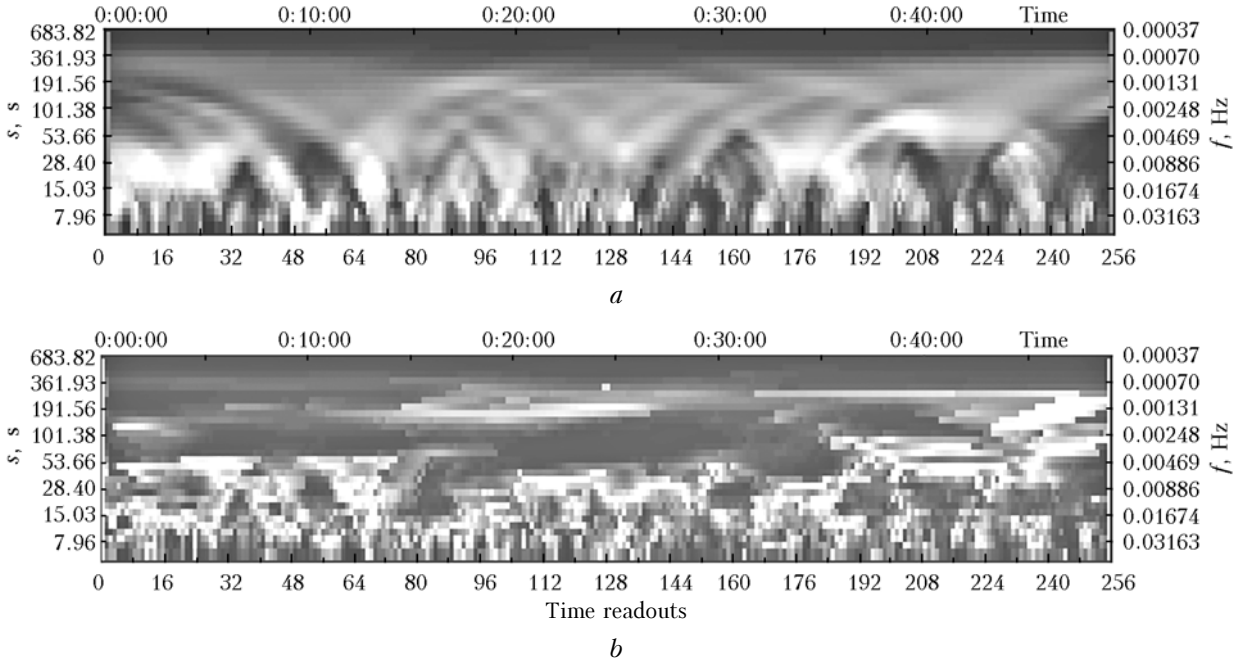

Fig. 9. Local coherence of the wavelet transforms of the signals V_1 and V_2 without (*a*) and with (*b*) phase adjustment.

This means that, once the local phase shifts are leveled, the velocity eddies of the corresponding scales, characterized by the high coherence, evolve within the time intervals synchronously with the constant (in time) phase difference, that is, they are coherent structures.

If we are interested in the behavior of the velocity eddies of a certain scale, then it is possible, selecting the corresponding scales in the plot of the local shifts and ignoring the others (that is, carrying out the local adjustment of the phase to the scales of the eddies), to determine the frequency–time intervals of coherence of these eddies using Eq. (3).

Thus, analyzing the space–time series of the wind velocity, measured at different altitudes (distances), it is possible to reveal regular components with the coordinated behavior, to estimate their scales, and to determine their time and frequency location. The procedure described can be used, obviously, not only for analyzing signals periodic in time, but also for estimating the period and velocity of propagation of individual wind perturbations. The approach proposed may appear useful when studying unsteady random processes, in particular, to reveal and investigate the dynamics of coherent formations in the atmosphere.

Acknowledgments

The authors are grateful to A.D. Ershov and A.V. Falits for the help in this work.

The work was supported, in part, by the Russian Foundation for Basic Research (Projects No. 03-05-64194-a and No. 06-05-64445-a).

References

1. J.S. Bendat and A.G. Piersol, *Random Data: Analysis and Measurement Procedures* (Wiley, New York, 1986).
2. N.L. Byzova, V.N. Ivanov, and M.K. Matskevich, Izv. Ros. Akad. Nauk, Fiz. Atmos. Okeana **32**, No. 3, 323–328 (1996).
3. G.N. Shur, Meteorol. Gidrol., No. 1, 5–11 (1994).
4. N.A. Bakas, P.J. Ioannou, and G.E. Kefaliakos, J. Atmos. Sci. **58**, 2790–2906 (2001).

5. S.V. Alekseenko, P.A. Kuibin, and V.L. Okulov, *Introduction to Theory of Concentrated Eddies* (Kutateladze Institute of Thermophysics SB RAS, Novosibirsk, 2003), 502 pp.
6. V.N. Ivanov and N.L. Byzova, Meteorol. Gidrol., No. 1, 5–25 (2001).
7. N.M. Astaf'eva, Izv. Vyssh. Uchebn. Zaved. PND **4**, No. 2, 3–39 (1996).
8. E. Terradellas, G. Morales, J. Cuxart, and C. Yagüc, Dyn. Atmos. and Oceans **34**, 225–244 (2001).
9. I.V. Petenko and V.A. Bezverkhnii, Meteorol. and Atmos. Phys. **71**, 195–216 (1999).
10. J.M. Ress, W.J. Staszewski, and J.R. Winkler, Dyn. Atmos. and Oceans **34**, 245–261 (2001).
11. I.V. Petenko, Boundary-Layer Meteorol. **100**, 287–299 (2001).
12. V.A. Bezverkhnii, Izv. Ros. Akad. Nauk, Fiz. Atmos. Okeana **37**, No. 5, 630–638 (2001).
13. V.A. Banakh, A.V. Falits, I.N. Smalikho, and S. Rahm, Atmos. Oceanic Opt. **18**, No. 12, 955–957 (2005).